Interface mismatch eigenstrain of non-slipping contacts between dissimilar elastic solids

Lifeng Ma[*1,2], Alexander M. Korsunsky[*3]

1. Department of Mechanical, Materials and Manufacturing Engineering, University of Nottingham, University Park, NG7 2RD, UK.

2. S&V Lab, Department of Engineering Mechanics, Xi'an Jiaotong University, 710049, Xi'an, China

3. Department of Engineering Science, University of Oxford, Oxford, OX1 3PJ, UK

Abstract

The problems of non-slipping contacts between dissimilar elastic solids are studied under the conditions of plane strain. When two dissimilar solids are incrementally pressed into contact, a relative tangential displacement along the contact interface emerges because of the material property mismatch. The spatial derivative of the relative tangential displacement is referred to as the interface mismatch eigenstrain, which is separately investigated according to the non-adhesive and adhesive surface conditions. The explicit solutions of the interface mismatch eigenstrain for non-slipping contacts with symmetrical indenter profiles are obtained, which enable a thorough analysis of the non-slipping contacts. These results provide the foundation for improved precision contact deformation modelling at the macro-, micro-, and nano- scales.

Keywords: Contact mechanics; non-slipping contact; interface mismatch eigenstrain; symmetric profile.

1. Introduction

The non-slipping contact can be simply described as below. When two bodies are brought into contact, pair-wise correspondence is established between points on the two surfaces that meet at the contact interface. Provided the level of friction is high enough, the two points will always maintain contact during subsequent incremental

---

[*] Corresponding authors

Email: Lifeng.Ma@nottingham.ac.uk, malf@mail.xjtu.edu.cn (LM); alexander.korsunsky@eng.ox.ac.uk (AMK); Tel.: +44 07542 773061

loading. The path of a surface particle entrained in a non-slipping contact is schematically illustrated in Fig. 1, where a contact between an elastic substrate and a rigid indenter is considered. Note that, apart from the readily apparent normal displacement induced by the indentation, a relative tangential displacement will also be spontaneously introduced and "frozen-in" along the contact interface, due to material property mismatch. The derivative of this displacement with respect to the lateral distance from the axis is referred to as the *interface mismatch eigenstrain* (Ma and Korsunsky, 2012), which is believed to reflect the strain's physical origin and characteristic of non-slipping contacts.
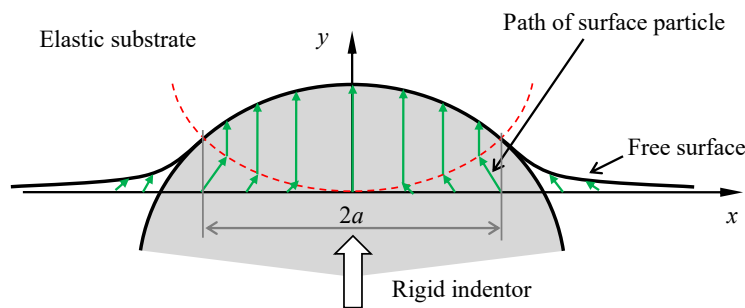

Fig. 1 Path of surface particle of non-slipping contact during incremental normal load (Adopted from the reference paper by Spence, 1968)

In order to improve the accuracy of modelling practical contact problems such as fretting fatigue (Nowell and Hills, 1988), nano-indentation (Borodich and Keer, 2004; Luan et al.,2006), bio-adhesion (Dartschet al., 1986; Yang and Saif, 2005; Ma and Korsunsky, 2012; Borodich et al., 2021), the non-slipping contact models were adopted in which the *interface mismatch eigenstrain* is taken into account. Apart from these practical requirements, more importantly, the study on non-slipping contact has evident theoretical significance in Contact Mechanics (Barber, 2018). The background to this study can be traced back to the work of Mossakovski (1954, 1963) and Goodman (1962). A frictional rigid-to-elastic axis-symmetric contact model with no slippage was initially studied. A step-by-step incremental approach was used, and the contact stresses were computed alongside the time evolution of the contact radius. Mossakovski presented the problems for a flat-ended cylinder and a parabolic punch. Goodman (1962) presented an approximate solution to the non-slipping Hertzian contact problem. The problems of this kind belong to the typical *elastic* mixed boundary-value problem. An important consideration arises concerning whether the solution should be independent of the load process. Spence (1968) proposed an

elegant self-similarity approach and made a significant contribution to this problem. He extended the range of rigid indenter profiles considered to include polynomials. Non-slipping contact problems then were formulated with an integral equation which can be solved using the Wiener-Hopf technique.

This approach was later on used to study the *symmetric* partial-slipping contact with the finite friction in the case of a two-dimensional problem (Spence, 1973; 1975). Spence found that the slip radius is the same for all power-law indenters and that the slip half-width is a function of the friction coefficient. If the friction is large enough, the analytical solution for fully non-slipping contacts can be obtained. Using the Wiener-Hopf technique, Zhupanska and Ulitko (2005) revisited this two-dimensional problem, and the exact solution to the problem of indentation with friction of a rigid cylinder into an elastic half-space was obtained in the form of an infinite series. It should be pointed out that when slipping is considered, the contact will be related to and dependent on the load history. The topic of interfacial slipping lies beyond the scope of the paper. Our attention is focused on the completely non-slipping contact problems.

For the non-slipping contacts, to find the *interface mismatch eigenstrain* plays a crucial role in entire process of solving problems. Soldatenkov (1996) has conducted an initial theoretical analysis for more general non-slipping elastic contact with rigid indenters. The contact gap function was represented in terms of a complicated functional transform, and a single complex-valued singular integral was formulated to specify the contact tractions. Clearly a direct and elaborate analysis on this problem needs to be carried on. Furthermore, at the micro- or nano- scale, the significant surface adhesive effect, i.e. the Van der Waals force, should be considered in contacts (Johnson et al., 1971). These small scale adhesion problems have been the subject of active research, e.g., in nano-indentation (Bhushan, 2017) and bio-adhesion (Arzt et al., 2003) studies. The deformation and traction distributions in adhesive non-slipping contacts will differ significantly from the ordinary non-slipping contacts at the macro-scale, which highlights the need for more careful consideration of the *interface mismatch eigenstrain* within them.

The aims of the present study are: (i) to seek the explicit solutions for the *interface mismatch eigenstrain* of non-slipping contacts with symmetrically profiled indenters, separately for non-adhesion and adhesion conditions; (ii) to extend the conventional *rigid-to-elastic* contact models found in the literature to a general

elastic-to-elastic non-slipping contact model, striving for a broader application; (iii) to present example solutions of non-slipping contacts such as e.g., for wedge and parabolic indenters. It is expected that this study may shed some light on all kinds of contacts where non-slipping conditions are observed.

The remainder of this paper is constructed in the following steps. In § 2, the basic knowledge on two-dimensional contact, boundary conditions, and external load conditions are presented. In § 3, a dissimilar elastic-elastic contact model without adhesion is formulated in terms of the Kolosov-Muskhelishvili complex formulae, and the *interface mismatch eigenstrain* is derived with the so-called consistency condition. Then the solutions for contacts with wedge and parabolic indenters are deduced in § 4. Similarly, in § 5, a dissimilar elastic-elastic *adhesive* contact model is formulated, and the corresponding *interface mismatch eigenstrain* is derived, with the assumption of constant stress intensity factor at the contact edges. The pull-off force is examined and the wedge and parabolic contacts are exemplified as an implementation. Finally, a concise summary is given in § 6.

2. Preliminary formulae for dissimilar contact

2.1 The Kolosov-Muskhelishvili complex potential formulae

In the Kolosov-Muskhelishvili complex formulation of plane elasticity, all components of stress and displacement can be expressed in terms of two Kolosov-Muskhelishvili complex potentials $\phi(z)$ and $\psi(z)$. Here we express them, alternatively, with $\Phi(z) = \phi'(z)$, $\Omega(z) = \left[z\phi'(z) + \psi(z) \right]'$ as follows (Muskhelishvili, 1953),

$$\sigma_{11} + \sigma_{22} = 2\left[\Phi(z) + \overline{\Phi(z)} \right]$$
$$\sigma_{22} - i\sigma_{12} = \Phi(z) + \overline{\Omega(z)} + (z - \bar{z})\overline{\Phi'(z)} \qquad , \qquad (2.1)$$
$$2\mu\left(u_{1,1} + iu_{2,1} \right) = \kappa\Phi(z) - \left[\overline{\Omega(z)} + (z - \bar{z})\overline{\Phi'(z)} \right]$$

where, $i = \sqrt{-1}$, $z = x_1 + ix_2 (= x + iy)$, $\Phi'(z) = d\Phi(z)/dz$, μ is shear modulus, the Kolosov constant $\kappa = 3 - 4\nu$ for plane strain, ν is Poisson's ratio, the comma followed by a subscript *i* indicates differentiation with respect to x_i, and the bar over a function denotes its complex conjugate. The Kolosov-Muskhelishvili complex potential formulae for contact problems have been extensively studied in literatures (see, e.g. Muskhelishvili, 1953; Galin, 1953; England, 1971; Gladwell, 1980; Hills et

al., 1993), but it is always confined within the *rigid-to-elastic* contact models. The present authors (Ma and Korsunsky, 2012) have extended this formula to the *elastic-to-elastic* contact models as shown in Fig. 2, by the continuity of traction along *x*-axis as

$$\left(\sigma_{22}-i\sigma_{12}\right)=\begin{cases}\left(\sigma_{22}-i\sigma_{12}\right)_{\#1}=\left(\sigma_{22}-i\sigma_{12}\right)_{\#2}, & |x|\leq a \\ 0, & |x|>a\end{cases}, \tag{2.2}$$

where *a* is the contact half-width, the subscripts '#1' and '#2' refer to the tractions respectively on the upper and lower surfaces. Its expression is as follows

$$\Phi(z)=\begin{cases}\Phi_1(z)=H(z), & z\in\#1 \\ \Phi_2(z)=-H(z), & z\in\#2\end{cases}, \quad \Omega(z)=\begin{cases}\Omega_1(z)=-\overline{H}(z), & z\in\#1 \\ \Omega_2(z)=\overline{H}(z), & z\in\#2\end{cases}, \tag{2.3}$$

where, small size of the contact area compared to the dimensions of the contacting bodies and their relative radii of curvature is assumed; $\Phi_1(z),\Omega_1(z)$ and $\Phi_1(z)$, $\Omega_2(z)$ denote the potentials for Solid #1 and Solid #2 respectively; all potentials are expressed in terms of one holomorphic function $H(z)$.
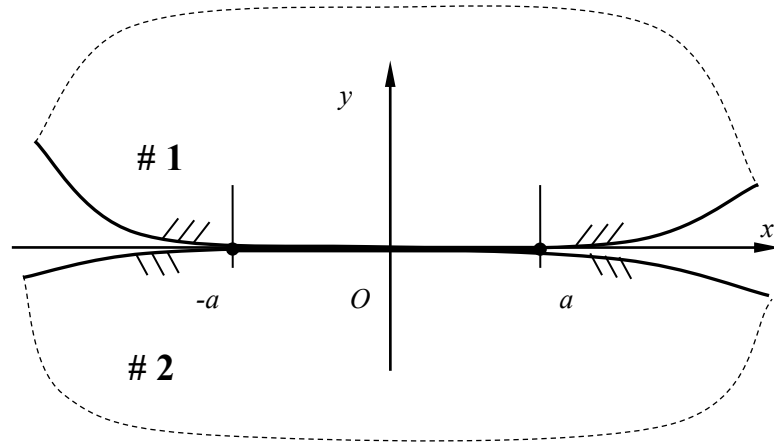

Fig. 2. Schematic diagram of a two-dimensional dissimilar contact, where #1 and #2 denote the upper and lower solids, respectively.

2.2 Contact boundary conditions

The boundary conditions to specify contact solution are listed below:

(i) Contact displacement condition. When two bodies are pressed together, deformation must occur so that the deformed bodies conform within the contact. The difference between the displacement derivatives of the two surfaces, with respect to the lateral coordinate (*x*-axis) within the contact surface, can be evaluated as

$$\left(\Delta u_{1,1}+i\Delta u_{2,1}\right)=\left(u_{1,1}+iu_{2,1}\right)_{upper\ surface}-\left(u_{1,1}+iu_{2,1}\right)_{lower\ surface}=g(x)+if(x),|x|<a.(2.4)$$

For general cases, the function $f(x)$ is directly determined by the profiles of the two contact bodies, but the function $g(x)$ is difficult to specify. For non-slipping symmetric contacts, the function $g(x)$ is always an even function and the function $f(x)$ is anti-symmetric odd function. The function $g(x)$ is the *interface mismatch eigenstrain* we mentioned before, which is to be determined.

(ii) Remote loading condition. To solve the boundary value problem, remote loading condition must be known, so that the contact width *2a* may be determined. The external load equals to the resultant force of interfacial traction given by

$$F_2-iF_1=\int_{-a}^{a}\left(\sigma_{22}-i\sigma_{12}\right)dx.\tag{2.5}$$

(iii) Traction behavior at contact edges. For the non-slipping contact with no adhesion, we suppose that the traction at the edges will vanish, while for the non-slipping contact with adhesion, we suppose that the traction at the edges will be singular. These conditions will be used to choose the branch functions to determine the contact traction behavior in following Sections.

Then by use of these conditions, we may specify the function $H(x)$. Once the complex function $H(x)$ is obtained, the deformation states of the two contacting bodies are ready to be solved through Eqs. (2.3) and (2.1).

3. The interface mismatch eigenstrain in non-slipping contact

For non-slipping contacts, the following condition pertains

$$\frac{\partial}{\partial a}\left[g(x)+if(x)\right]=0,\quad\left(|x|<a\right)\tag{3.1}$$

which means that the function $f(x)$ and the *interface mismatch eigenstrain* $g(x)$ within the non-slipping contact is independent of the variation of contact width *2a*. This condition is crucial to fix the function $g(x)$.

3. 1 Complex potential for the contact

Eq. (2.4) can be represented from the third equation of (2.1) and further be expressed in terms of the solution (2.3) as

$$H(x^+)+\left(\frac{1+\beta}{1-\beta}\right)H(x^-)=\frac{2\mu_1\mu_2}{\kappa_1\mu_2+\mu_1}\left[g(x)+if(x)\right]=\frac{\left[g(x)+if(x)\right]}{A(1-\beta)},\tag{3.2}$$

where, superscripts '+' and '−' respectively stand for the limits $y \to 0^+$ and $y \to 0^-$, the compliance parameter A and the Dundurs' parameter β are used, given by

$$A = \frac{(\kappa_1 + 1)}{4\mu_1} + \frac{(\kappa_2 + 1)}{4\mu_2}, \quad \beta = \frac{\mu_1(\kappa_2 - 1) - \mu_2(\kappa_1 - 1)}{\mu_1(\kappa_2 + 1) + \mu_2(\kappa_1 + 1)}, \tag{3.3}$$

and subscripts 1 and 2 refer to the two materials. Since the traction at the two contact edges vanishes for non-slipping contact with no adhesion, it is reasonable to choose a branch function (Hills et al., 1993)

$$X(z) = (z + a)^\delta (z - a)^{1-\delta} \tag{3.4}$$

where

$$\delta = \frac{1}{2} - i\varepsilon, \quad \varepsilon = \frac{1}{2\pi} \ln \frac{(1-\beta)}{(1+\beta)}. \tag{3.5}$$

So that Eq. (3.2) can be rewritten as

$$\frac{H(x^+)}{X(x^+)} - \frac{H(x^-)}{X(x^-)} = \frac{1}{X(x^+)} \frac{[g(x) + if(x)]}{A(1-\beta)} \tag{3.6}$$

in which the properties

$$\begin{aligned} X(x^+) &= ie^{-\pi\varepsilon}(x+a)^\delta(a-x)^{1-\delta} \\ X(x^-) &= -ie^{\pi\varepsilon}(x+a)^\delta(a-x)^{1-\delta} \end{aligned} \tag{3.7}$$

are used. Eq. (3.6) is a standard Hilbert equation and its solution is

$$H(z) = \frac{1}{A(1-\beta)} \frac{X(z)}{2\pi i} \int_{-a}^{a} \frac{[g(t) + if(t)]}{X(t^+)} \frac{dt}{t - z}. \tag{3.8}$$

The *interface mismatch eigenstrain* $g(x)$ is to be determined below.

3.2 Interface mismatch eigenstrain

The *interface mismatch eigenstrain* $g(x)$ can be specified by the following consistency condition (Muskhelishvili, 1953; Hills et al., 1993)

$$0 = \int_{-a}^{a} \frac{g(t) + if(t)}{X(t^+)} dt = \int_{-1}^{1} \frac{g(aT) + if(aT)}{ie^{-\pi\varepsilon}(T+1)^\delta(1-T)^{1-\delta}} dT. \tag{3.9}$$

This condition indeed is an assumption for traction behavior at contact edges for non-adhesive contacts we mentioned in sub-Section 2.2. This ensures that both tractions $\sigma_{22}(x,0)$ and $\sigma_{12}(x,0)$ along the contact surface simultaneously vanish at the two contact ends (points $x = \pm a$). It should be emphasized that the condition (3.9)

intrinsically attaches the unknown function $g(t)$ to the given function $f(t)$, resulting in an expression potentially to be fixed. Because $f(x)$ is an anti-mirror-symmetric odd function and $g(t)$ is a mirror-symmetric even function with respect to y-axis, they can be expressed in series as

$$\begin{cases} f(t) = f(aT) = \sum_{n=0}^{\infty} c_n \operatorname{sgn}(T^{n+1})(aT)^n = \sum_{n=0}^{\infty} c_n \operatorname{sgn}(T^{n+1}) T^n a^n \\ g(t) = g(aT) = \sum_{n=0}^{\infty} d_n \operatorname{sgn}(T^n)(aT)^n = \sum_{n=0}^{\infty} d_n |T|^n a^n \end{cases}, (-1 < T < 1) \quad (3.10)$$

where c_n and d_n are constants. The evident advantages of expression (3.10) are that each term at the same order may independently represents a contact case, and at the same time, the entire series can be understood as two Tylor's expansions, respectively, for any functions $f(t)$ and $g(t)$ with respect to the origin.

Inserting the representative terms $c_n \operatorname{sgn}(T^{n+1}) T^n a^n$ and $d_n |T|^n a^n$ in Eqs. (3.10) into (3.9), we can get

$$0 = \int_{-a}^{a} \frac{g(t) + if(t)}{X(t^+)} dt = \left[\int_{-1}^{1} \frac{d_n |T|^n + ic_n \operatorname{sgn}(T^{n+1}) T^n}{(T+1)^{\delta} (1-T)^{1-\delta}} dT \right] a^n, \quad (n = 0,1,2,3). \quad (3.11)$$

Eq. (3.11) is held for any value of a, which actually requires

$$0 = \int_{-1}^{1} \frac{d_n |T|^n + ic_n \operatorname{sgn}(T^{n+1}) T^n}{(1+T)^{\delta} (1-T)^{1-\delta}} dT, \quad (n = 0,1,2,3....). \quad (3.12)$$

This implies that

$$d_n = \Upsilon_n c_n, \quad (n = 0,1,2,3) \quad (3.13)$$

where

$$\Upsilon_n = -i \left(\int_{-1}^{1} \frac{\operatorname{sgn}(T^{n+1}) T^n}{(1+T)^{\delta} (1-T)^{1-\delta}} dT \right) \left(\int_{-1}^{1} \frac{|T|^n}{(1+T)^{\delta} (1-T)^{1-\delta}} dT \right)^{-1}. \quad (3.14)$$

In view of Eq. (3.5), we can find

$$\begin{aligned} (T+1)^{\delta} (1-T)^{(1-\delta)} &= (T+1)^{\frac{1}{2}} (1-T)^{\frac{1}{2}} \left(\cos \varepsilon \ln \left(\frac{T+1}{1-T} \right) - i \sin \varepsilon \ln \left(\frac{T+1}{1-T} \right) \right) \\ (1-T)^{\delta} (1+T)^{(1-\delta)} &= (1+T)^{\frac{1}{2}} (1-T)^{\frac{1}{2}} \left(\cos \varepsilon \ln \left(\frac{T+1}{1-T} \right) + i \sin \varepsilon \ln \left(\frac{T+1}{1-T} \right) \right) \end{aligned}. \quad (3.15)$$

By using Eq. (3.15), Eq. (3.14) can be written in to a standard form as

8

$$\Upsilon_n = \Upsilon_n(\varepsilon) = \frac{\int_0^1 \sin\left(\varepsilon \ln \frac{T+1}{1-T}\right) \frac{T^n}{\sqrt{1-T^2}} dT}{\int_0^1 \cos\left(\varepsilon \ln \frac{T+1}{1-T}\right) \frac{T^n}{\sqrt{1-T^2}} dT}. \qquad (n=0,1,2,3...) \qquad (3.16)$$

This is one of the key results obtained in this paper. It is important to note that for an arbitrary bi-material combination $|\beta| \le 1/2$, and from Eq. (3.5) we may find $|\varepsilon| \le \frac{1}{2\pi} \ln(3) \approx 0.1784$. By virtue of Eq. (3.16), the approximate value of Υ_n for different number n can be obtained as follows.

$$\begin{cases} \Upsilon_0 = \Upsilon_0(\varepsilon) = \dfrac{8\text{Catalan}}{\pi}\varepsilon + O(\varepsilon)^3 \approx 2.3325\ \varepsilon \\[2mm] \Upsilon_1 = \Upsilon_1(\varepsilon) = \pi\varepsilon + O(\varepsilon)^3 \approx 3.1416\ \varepsilon \\[2mm] \Upsilon_2 = \Upsilon_2(\varepsilon) = \dfrac{4(1+2\text{Catalan})}{\pi}\varepsilon + O(\varepsilon)^3 \approx 3.6057\varepsilon \\[2mm] \Upsilon_3 = \Upsilon_3(\varepsilon) = \dfrac{5\pi}{4}\varepsilon + O(\varepsilon)^3 \approx 3.9270\ \varepsilon \\[2mm] \Upsilon_i = \Upsilon_i(\varepsilon) = ... \end{cases} \qquad (3.17)$$

where Catalan is referred to as the Catalan's constant

$$\text{Catalan} = \sum_{m=0}^{\infty} \frac{(-1)^n}{(2n+1)^2} = 0.915965594177219015.... \qquad (3.18)$$

It can be interestingly found that the correlation coefficient Υ_n is gradually increasing with the order of the indenter profile function, for a fixed bi-material combination.

4. Non-slipping contacts

Owing to the expression of *interface mismatch eigenstrain* in hand, the general solution for non-slipping contact can be straightforward derived, and then two typical contact models - with wedge and parabola indenters will be constructed.

4.1 General solution for non-slipping contact

To derive the traction distribution along the contact interface, from Eq. (3.8) one has

$$\begin{aligned} H(x^+) &= \frac{X(x^+)}{A(1-\beta)}\left[\frac{1}{2\pi i}\int_{-a}^{a} \frac{g(t)+if(t)}{X(t^+)}\frac{1}{t-x}dt + \frac{1}{2}\frac{g(x)+if(x)}{X(x^+)} \right], \\ H(x^-) &= \frac{X(x^-)}{A(1-\beta)}\left[\frac{1}{2\pi i}\int_{-a}^{a} \frac{g(t)+if(t)}{X(t^+)}\frac{1}{t-x}dt - \frac{1}{2}\frac{g(x)+if(x)}{X(x^+)} \right] \end{aligned} \qquad (4.1)$$

and then from Eqs. (2.1) and (2.3) the contact traction is given by

$$\sigma_{22} - i\sigma_{12} = H(x^+) - H(x^-)$$
$$= \frac{\beta\left[g(x)+if(x)\right]}{A(1-\beta^2)} - i\frac{(x+a)^\delta (a-x)^{1-\delta}}{A(1-\beta^2)\pi} \int_{-a}^{a} \frac{\left[g(t)+if(t)\right]}{(a-t)^{(1-\delta)}(t+a)^\delta} \frac{1}{(t-x)}dt \qquad (4.2)$$

With the aid of Eqs. (A2) and (3.5), after a straightforward manipulation, Eq. (4.2) can be rewritten as

$$\sigma_{22} - i\sigma_{12} = -i\left\{ \frac{(x+a)^\delta (a-x)^{1-\delta}}{A(1-\beta^2)} \frac{1}{\pi}\int_{-a}^{a} \frac{\left[g(t)+if(t)\right]-\left[g(x)+if(x)\right]}{(a-t)^{(1-\delta)}(t+a)^\delta (t-x)}dt \right\}. \qquad (4.3)$$

Inserting $\delta = \dfrac{1}{2} - i\varepsilon$ into (4.3) leads to

$$\sigma_{22} - i\sigma_{12} = -i\left\{ \frac{(x+a)^{\frac{1}{2}-i\varepsilon} (a-x)^{\frac{1}{2}+i\varepsilon}}{A(1-\beta^2)} \frac{1}{\pi}\int_{-a}^{a} \frac{\left[g(t)+if(t)\right]-\left[g(x)+if(x)\right]}{(a-t)^{\frac{1}{2}+i\varepsilon}(t+a)^{\frac{1}{2}-i\varepsilon}(t-x)}dt \right\}. \qquad (4.4)$$

It can be observed from Eq. (4.4) that: (*i*) the tractions decrease to zero as x approaches from one inner point within the contact surface to the two ends $\pm a$; (*ii*) at the same time, the tractions show an obvious oscillatory behavior as x approaches the two ends $\pm a$, which is quite like the one of an interface crack-tip. This behavior was first found by Abramov (Zhupanska and Ulitko, 2005).

Substituting Eqs. (4.2) into (2.5), exchanging the order of integrals, and with the aid of Eqs. (A2), (3.5), (3.9) and $(\beta + \tanh \pi\varepsilon) = 0$, after a straightforward manipulation, one can relate the external load as

$$F_2 - iF_1 = \int_{-a}^{a}(\sigma_{22}-i\sigma_{12})dx = -\frac{i\cosh\pi\varepsilon}{A}\int_{-a}^{a}\frac{\left[g(t)+if(t)\right]t}{(t+a)^\delta (a-t)^{1-\delta}}dt$$
$$= -\frac{i\cosh\pi\varepsilon}{A}\int_{-a}^{a}\frac{\left[g(t)+if(t)\right]t}{\sqrt{a^2-t^2}}\left(\frac{a+t}{a-t}\right)^{i\varepsilon}dt \qquad (4.5)$$

Furthermore, with consideration of the odevity of functions and the symmetry of integral domains, it follows

$$\begin{cases} F_1 = 0 \\ F_2 = \dfrac{\cosh\pi\varepsilon}{A}\displaystyle\int_{-a}^{a}\frac{1}{\sqrt{a^2-t^2}}\left[g(t)\sin\left(\varepsilon\ln\frac{a+t}{a-t}\right)+f(t)\cos\left(\varepsilon\ln\frac{a+t}{a-t}\right)\right]tdt \end{cases} \qquad (4.6)$$

Evidently, the *interface mismatch eigenstrain* is involved in the resultant force F_2. If $\beta = 0$, Eqs. (4.2) and (4.6) become, respectively, as

$$\sigma_{22} - i\sigma_{12} = -i\frac{\sqrt{a^2 - x^2}}{A\pi}\int_{-a}^{a}\frac{\left[g(t) + if(t)\right]}{\sqrt{a^2 - t^2}}\frac{1}{(t - x)}dt ,$$ (4.7)

$$\begin{cases} F_1 = 0 \\ F_2 = \dfrac{1}{A}\displaystyle\int_{-a}^{a}\frac{1}{\sqrt{a^2 - t^2}}f(t)t\,dt \end{cases}$$ (4.8)

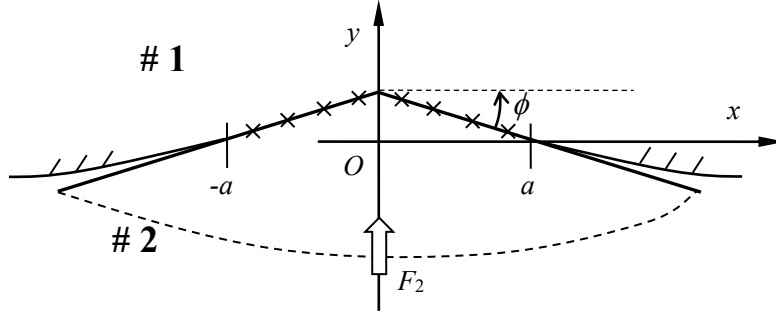*4.2 Non-slipping symmetric wedge contact*

Fig. 3 Non-slipping indentation of a semi-infinite plane by a wedge, in which #1 stands for the upper plane material and #2 stands for the lower plane material

As shown in Fig. 3, for the non-slipping wedge contact, Eq. (3.10) allows

$$\begin{cases} f(x) = c_0\,\mathrm{sgn}(x) = -\phi\,\mathrm{sgn}(x) \\ g(x) = d_0 = c_0\Upsilon_0 = -\phi\Upsilon_0 \end{cases}, \quad (|x| < a).$$ (4.9)

Inserting Eqs. (4.9) into (4.3) gives

$$\sigma_{22} - i\sigma_{12} = c_0\frac{(x+a)^\delta(a-x)^{1-\delta}}{A(1-\beta^2)}\frac{1}{\pi}\int_{-a}^{a}\frac{\left[\mathrm{sgn}(t) - \mathrm{sgn}(x)\right]}{(a-t)^{(1-\delta)}(t+a)^\delta(t-x)}dt, \quad (|x| < a)$$ (4.10)

Eq. (4.6) degenerates to

$$F_2 = 2\frac{\cosh\pi\varepsilon}{A}\left\{ d_0\int_0^a\frac{\sin\left(\varepsilon\ln\dfrac{a+t}{a-t}\right)}{(a^2 - t^2)^{\frac{1}{2}}}t\,dt + c_0\int_0^a\frac{\cos\left(\varepsilon\ln\dfrac{a+t}{a-t}\right)}{(a^2 - t^2)^{\frac{1}{2}}}t\,dt \right\}.$$ (4.11)

If $\beta = 0$, and ϕ is very small, Eqs. (4.10) and (4.11), respectively, degenerate to

$$\sigma_{22} - i\sigma_{12} = -\frac{2\phi}{\pi A}\cosh^{-1}(a/|x|), \quad (|x| < a)$$ (4.12)

and

$$F_2 = -\frac{2\phi}{A}a .$$ (4.13)

These degenerate results are completely consistent with the results for frictionless

results (Hills et al., 1993).

4.3 Non-slipping symmetric parabola contact

A non-slipping contact between a half-plane and a parabola as shown in Fig. 4 will be explored.
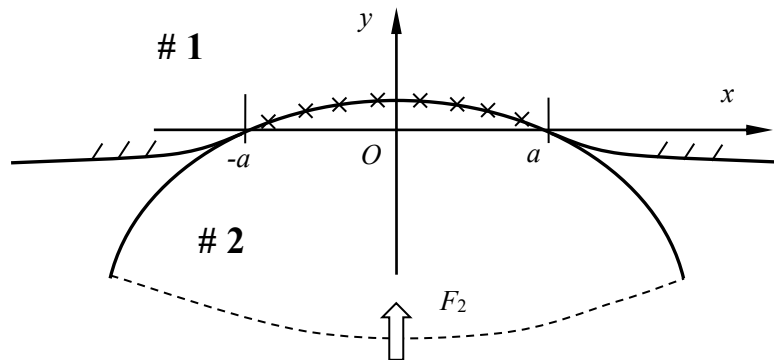

Fig. 4 Non-slipping contact between a semi-infinite plane and a parabola indenter, in which #1 stands for the upper plane material and #2 stands for the lower plane material

For this case, the functions $f(x)$ and $g(t)$ can be expressed as

$$\begin{cases} f(x) = c_1 x = -x/R \\ g(x) = d_1 |x| = -\Upsilon_1 |x|/R \end{cases}, \qquad (|x| < a) \tag{4.14}$$

Substituting Eqs. (4.14) into (4.3) and (4.6) leads to

$$\sigma_{22} - i\sigma_{12} = -i\left\{ \frac{(x+a)^{\delta}(a-x)^{1-\delta}}{A(1-\beta^2)} \frac{1}{\pi}\left[\int_{-a}^{a} \frac{d_1(|t|-|x|)}{(a-t)^{(1-\delta)}(t+a)^{\delta}(t-x)} dt + \frac{ic_1\pi}{\cosh \pi\varepsilon} \right] \right\}, \tag{4.15}$$

$$F_2 = \frac{\cosh \pi\varepsilon}{A} \int_{-a}^{a} \frac{d_1|t|\sin\left(\varepsilon \ln \dfrac{a+t}{a-t}\right) + c_1 t \cos\left(\varepsilon \ln \dfrac{a+t}{a-t}\right)}{(t+a)^{\frac{1}{2}}(a-t)^{\frac{1}{2}}} t\,dt \tag{4.16}$$

If $\beta = 0$, Eqs. (4.15) and (4.16), respectively, degenerate to

$$\sigma_{22} - i\sigma_{12} = \frac{c_1}{A}\sqrt{a^2 - x^2} = -\frac{\sqrt{a^2 - x^2}}{AR}, \tag{4.17}$$

$$F_2 = \frac{c_1}{A}\frac{a^2}{2}\pi = -\frac{\pi a^2}{2AR}. \tag{4.18}$$

These degenerate results are can be found in literature (Barber, 2018).

5. Non-slipping adhesive contact

Following the Hertzian contact assumptions (Hertz, 1881), the well-known JKR model has been proposed to deal with the adhesion problems (Johnson et al., 1971), in which the frictionless contact assumption is inherited. To adopt the *interface mismatch eigenstrain* in non-slipping contact without adhesion to the corresponding non-slipping adhesive contacts, at present, seems not appropriate. This is because the interface tangential action is taken into account and the boundary conditions for the two scenarios are far different. Thus, the *interface mismatch eigenstrain* in non-slipping adhesive contact should be alternatively sought first. Similar to the JKR contact model, the contact traction near the contact edges is supposed to be singular, and the contact width will be determined by the combination of the Griffith energy balance near the contact edge and external load.

5. 1 General solution

As already derived in subsection 3.1, the equation concerned with the undetermined function $H(z)$ as Eq. (3.2) is

$$H(x^+) + \left(\frac{1+\beta}{1-\beta}\right) H(x^-) = \frac{[g(x)+if(x)]}{A(1-\beta)}. \tag{5.1}$$

Since the traction at the two contact edges is singular for non-slipping adhesive contact, this time we employ the branch function (Hills et al., 1993)

$$X(z) = (z+a)^{-\delta} (z-a)^{-(1-\delta)} \tag{5.2}$$

where

$$\delta = \frac{1}{2} + i\varepsilon, \quad \varepsilon = \frac{1}{2\pi} \ln \frac{(1-\beta)}{(1+\beta)}, \tag{5.3}$$

so as to find $H(z)$. It should be pointed out that the expression for δ in Eq. (5.3) is different from the one in Eq. (3.5). Of course, this branch function will result in a singular traction at the two contact edges. By use of

$$\begin{aligned} X(t^+) &= (t+a)^{-\delta} (a-t)^{\delta-1} (-i) e^{-\varepsilon\pi} \\ X(t^-) &= (t+a)^{-\delta} (a-t)^{\delta-1} i e^{\varepsilon\pi} \end{aligned} \quad , |t| < a \tag{5.4}$$

Eq. (5.1) can be rewritten as

$$\frac{H(x^+)}{X(x^+)} - \frac{H(x^-)}{X(x^-)} = \frac{1}{X(x^+)} \frac{[g(x)+if(x)]}{A(1-\beta)}. \tag{5.5}$$

The solution to Eq. (5.5) is

$$H(z) = X(z)\left[\frac{1}{A(1-\beta)}\frac{1}{2\pi i}\int_{-a}^{a}\frac{g(t)+if(t)}{X(t^+)}\frac{1}{t-z}dt + P\right] \qquad (5.6)$$

The constant complex number $P(= P_2 - iP_1)$ and the contact half-width a are to be determined below.

From Eq. (5.6), one has

$$H(x^-) = X(x^-)\left[\frac{1}{A(1-\beta)}\left(\frac{1}{2\pi i}\int_{-a}^{a}\frac{g(t)+if(t)}{X(t^+)}\frac{1}{t-x}dt - \frac{1}{2}\frac{g(x)+if(x)}{X(x^+)}\right) + P\right]$$

$$H(x^+) = X(x^+)\left[\frac{1}{A(1-\beta)}\left(\frac{1}{2\pi i}\int_{-a}^{a}\frac{g(t)+if(t)}{X(t^+)}\frac{1}{t-x}dt + \frac{1}{2}\frac{g(x)+if(x)}{X(x^+)}\right) + P\right]$$

(5.7)

Similarly, the contact traction along the interface from Eqs. (2.1), (2.3) and (5.7) is

$$\sigma_{22} - i\sigma_{12} = H(x^+) - H(x^-)$$
$$= \frac{\beta[g(x)+if(x)]}{A(1-\beta^2)} - \frac{2(x+a)^{-\delta}(a-x)^{\delta-1}e^{\varepsilon\pi}(iP_2+P_1)}{(1-\beta)} \qquad (5.8)$$
$$-i\frac{(a-x)^{\delta-1}(x+a)^{-\delta}}{A(1-\beta^2)}\frac{1}{\pi}\int_{-a}^{a}\frac{(t+a)^{\delta}(a-t)^{1-\delta}[g(t)+if(t)]}{t-x}dt$$

This is a general solution for the interface traction of non-slipping adhesive contact. The external load equals to the resultant force of interfacial traction given by

$$F_2 - iF_1 = \int_{-a}^{a}(\sigma_{22}-i\sigma_{12})dx$$
$$= \int_{-a}^{a}\frac{\beta[g(x)+if(x)]}{A(1-\beta^2)}dx - \frac{2e^{\varepsilon\pi}(iP_2+P_1)}{(1-\beta)}\int_{-a}^{a}(x+a)^{-\delta}(a-x)^{\delta-1}dx \qquad (5.9)$$
$$-i\int_{-a}^{a}\left(\frac{(a-x)^{\delta-1}(x+a)^{-\delta}}{A(1-\beta^2)}\frac{1}{\pi}\int_{-a}^{a}\frac{(t+a)^{\delta}(a-t)^{1-\delta}[g(t)+if(t)]}{t-x}dt\right)dx$$

By exchanging the order of integration in the third term, and considering Eqs. (A2) and $(\beta+\tanh\pi\varepsilon)=0$, Eq. (5.9) can be simplified to

$$F_2 - iF_1 = \int_{-a}^{a}(\sigma_{22}-i\sigma_{12})dx = -2\pi(iP_2+P_1). \qquad (5.10)$$

Since this contact is a symmetric contact, $F_1 = 0$, so that $P_2 = 0$ in Eq. (5.10). Then Eq. (5.8) can be rewritten as

$$\sigma_{22} - i\sigma_{12} = H\left(x^+\right) - H\left(x^-\right)$$

$$= \frac{\beta\left[g(x) + if(x)\right]}{A\left(1-\beta^2\right)} + \frac{F_2 e^{\varepsilon\pi}}{\pi\left(1-\beta\right)}\left(x+a\right)^{-\delta}\left(a-x\right)^{\delta-1} \qquad . \quad (5.11)$$

$$-i\frac{\left(a-x\right)^{\delta-1}\left(x+a\right)^{-\delta}}{A\left(1-\beta^2\right)}\frac{1}{\pi}\int_{-a}^{a}\frac{\left(t+a\right)^{\delta}\left(a-t\right)^{1-\delta}\left[g(t)+if(t)\right]}{t-x}dt$$

5.2 Stress intensity factor and interface mismatch eigenstrain

As mentioned before, the stress distribution behavior at the edge of non-slipping dissimilar adhesive contact is always singular as the one of an interfacial crack tip. The stress intensity factor at the reversible contact edge (see Fig. 1) is supposed to be always equal to a constant critical value in non-slipping adhesive contact, namely,

$$\begin{cases} K_L = \lim_{x\to -a^+}\sqrt{2\pi}\left(x+a\right)^{\delta}\left(\sigma_{22} - i\sigma_{12}\right) = K_c \\ K_R = \lim_{x\to a^-}\sqrt{2\pi}\left(a-x\right)^{1-\delta}\left(\sigma_{22} - i\sigma_{12}\right) = \bar{K}_c \end{cases} . \qquad (5.12)$$

where K_c is a constant number for a specific material combination. This assumption plays a crucial role in adhesive contact as the consistency condition (3.9) for non-adhesive contacts. It should be explained here that if there is no this assumption, the boundary conditions presented in Sub-section 2.2 are not sufficient to solve this contact problem.

By substituting Eq. (5.11) into the first equation of (5.12), it follows

$$K_c = \sqrt{2\pi}\left(2a\right)^{\delta-1}\left\{\frac{F_2 e^{\varepsilon\pi}}{\pi\left(1-\beta\right)} - i\frac{1}{A\left(1-\beta^2\right)}\frac{1}{\pi}\int_{-a}^{a}\frac{\left(t+a\right)^{\delta}\left(a-t\right)^{1-\delta}\left[g(t)+if(t)\right]}{t+a}dt\right\}$$

$$= \sqrt{2\pi}\left(2a\right)^{\delta-1}\left\{\frac{F_2 e^{\varepsilon\pi}}{\pi\left(1-\beta\right)} - i\frac{a}{A\left(1-\beta^2\right)}\frac{1}{\pi}\int_{-1}^{1}\frac{\left(T+1\right)^{\delta}\left(1-T\right)^{1-\delta}\left[g(aT)+if(aT)\right]}{\left(T+1\right)}dT\right\} \qquad . (5.13)$$

Considering Eq. (3.10) and, for convenience, taking the representative terms $c_n\,\mathrm{sgn}\left(T^{n+1}\right)T^n a^n$ and $d_n\left|T\right|^n a^n$ in (3.10) into (5.13), we have

$$K_c = \sqrt{2\pi}\left(2a\right)^{\delta-1}\left\{\frac{F_2 e^{\varepsilon\pi}}{\pi\left(1-\beta\right)} - i\frac{a^{n+1}}{A\left(1-\beta^2\right)}\frac{1}{\pi}\int_{-1}^{1}\frac{\left(T+1\right)^{\delta}\left(1-T\right)^{1-\delta}\left[d_n\left|T\right|^n + ic_n\,\mathrm{sgn}\left(T^{n+1}\right)T^n\right]}{\left(T+1\right)}dT\right\}. (5.14)$$

Taking derivative of two sides of Eq. (5.14) by a yields

$$0 = \frac{\left(\delta-1\right)F_2 e^{\varepsilon\pi}}{\pi\left(1-\beta\right)} + \frac{a e^{\varepsilon\pi}}{\pi\left(1-\beta\right)}\frac{\partial F_2}{\partial a} - i\frac{\left(\delta+n\right)a^{n+1}}{A\left(1-\beta^2\right)}\frac{1}{\pi}\int_{-1}^{1}\frac{\left(T+1\right)^{\delta}\left(1-T\right)^{1-\delta}\left[d_n\left|T\right|^n + ic_n\,\mathrm{sgn}\left(T^{n+1}\right)T^n\right]}{\left(T+1\right)}dT \,.$$

$$(5.15)$$

At the critical pull-off moment (namely, $\partial F_2/\partial a = 0$), the pull-off force can be expressed as

$$F_{2c} = i\frac{(\delta+n)a_c^{n+1}}{(\delta-1)Ae^{\varepsilon\pi}(1+\beta)}\int_{-1}^{1}\frac{(T+1)^{\delta}(1-T)^{1-\delta}\left[d_n|T|^n+ic_n\,\mathrm{sgn}(T^{n+1})T^n\right]}{(T+1)}dT,$$
(5.16)

where a_c is the corresponding contact half-width at the pull-off moment. Eq. (5.16) actually exerts a constraint to d_n. Namely, the left-hand side of Eq. (5.16) is a real number and thus the imaginary part of the right hand side must vanish. In order to separate the imaginary part and real part, after a straightforward manipulation, Eq. (5.16) can be rewritten as

$$F_{2c} = \frac{2a_c^{n+1}\cosh\pi\varepsilon}{\left(\varepsilon^2+\frac{1}{4}\right)A}\left\{\begin{bmatrix}(1+n)\varepsilon\int_0^1\left[d_n\cos\left(\varepsilon\ln\frac{T+1}{1-T}\right)-c_n\sin\left(\varepsilon\ln\frac{T+1}{1-T}\right)\right]\frac{T^n}{\sqrt{1-T^2}}dT \\ +\left(\varepsilon^2-\frac{1}{4}-\frac{1}{2}n\right)\int_0^1\left[c_n\cos\left(\varepsilon\ln\frac{T+1}{1-T}\right)+d_n\sin\left(\varepsilon\ln\frac{T+1}{1-T}\right)\right]\frac{T^{n+1}}{\sqrt{1-T^2}}dT\end{bmatrix} \\ +i\begin{bmatrix}\left(\varepsilon^2-\frac{1}{4}-\frac{1}{2}n\right)\int_0^1\left[d_n\cos\left(\varepsilon\ln\frac{T+1}{1-T}\right)-c_n\sin\left(\varepsilon\ln\frac{T+1}{1-T}\right)\right]\frac{T^n}{\sqrt{1-T^2}}dT \\ -(1+n)\varepsilon\int_0^1\left[c_n\cos\left(\varepsilon\ln\frac{T+1}{1-T}\right)+d_n\sin\left(\varepsilon\ln\frac{T+1}{1-T}\right)\right]\frac{T^{n+1}}{\sqrt{1-T^2}}dT\end{bmatrix}\end{bmatrix}\right\}.$$
(5.17)

Because the imaginary part is equal to 0, the parameter d_n can be identified from Eq. (5.17) as

$$d_n = \vartheta_n c_n, \qquad (n = 0,1,2,3....)$$
(5.18)

where

$$\vartheta_n = \frac{\int_0^1\left[\sin\left(\varepsilon\ln\frac{T+1}{1-T}\right)\right]\frac{T^n}{\sqrt{1-T^2}}dT + \frac{(1+n)\varepsilon}{\left(\varepsilon^2-\frac{1}{4}-\frac{1}{2}n\right)}\int_0^1\left[\cos\left(\varepsilon\ln\frac{T+1}{1-T}\right)\right]\frac{T^{n+1}}{\sqrt{1-T^2}}dT}{\int_0^1\left[\cos\left(\varepsilon\ln\frac{T+1}{1-T}\right)\right]\frac{T^n}{\sqrt{1-T^2}}dT - \frac{(1+n)\varepsilon}{\left(\varepsilon^2-\frac{1}{4}-\frac{1}{2}n\right)}\int_0^1\left[\sin\left(\varepsilon\ln\frac{T+1}{1-T}\right)\right]\frac{T^{n+1}}{\sqrt{1-T^2}}dT}.$$
(5.19)

The approximate value of ϑ_n for different n number can be obtained as follows.

$$\begin{cases}\vartheta_0 = \vartheta_0(\varepsilon) = \dfrac{8(\mathrm{Catalan}-1)}{\pi}\varepsilon+O(\varepsilon)^3 \approx -0.2140\,\varepsilon \\[3mm] \vartheta_1 = \vartheta_1(\varepsilon) = \dfrac{\pi}{3}\varepsilon+O(\varepsilon)^3 \approx 1.0472\,\varepsilon \\[3mm] \vartheta_2 = \vartheta_2(\varepsilon) = \dfrac{4(10\mathrm{Catalan}-3)}{5\pi}\varepsilon+O(\varepsilon)^3 \approx 1.5685\,\varepsilon\,. \\[3mm] \vartheta_3 = \vartheta_3(\varepsilon) = \dfrac{17\pi}{28}\varepsilon+O(\varepsilon)^3 \approx 1.9074\,\varepsilon \\[3mm] \vartheta_i = \vartheta_i(\varepsilon) = ...\end{cases}$$
(5.20)

5.3 Pull-off force

It should be noted that Eq. (5.16) also satisfies Eq. (5.14) at the pull-off moment, and thus combining them together leads to

$$K_c = \sqrt{2\pi} \left(2a_c\right)^{\delta-1} \frac{e^{\varepsilon\pi}}{\pi} \frac{1}{\left(1-\beta\right)} \frac{\left(1+n\right)}{\left(\delta+n\right)} F_{2c}. \tag{5.21}$$

By employing the Griffith energy balance at the interfacial crack tip (Malyshev and Salganik, 1965), the interface surface energy at the adhesive contact edge can be written in terms of stress intensity factor as

$$\gamma = \frac{A}{4\cosh^2 \pi\varepsilon} \left|K_c\right|^2 = \frac{A\left(1-\beta^2\right)}{4} K_c \overline{K}_c = \frac{A\left(1+n\right)^2}{4\pi a_c \left(\delta+n\right)\left(\overline{\delta}+n\right)} \left(F_{2c}\right)^2, \tag{5.22}$$

where γ is the interface surface energy. Thus, the critical contact half-width at the pull-off moment can be resolved from Eq. (5.22) as

$$a_c = \frac{A\left(1+n\right)^2}{4\pi\gamma\left(\delta+n\right)\left(\overline{\delta}+n\right)} \left(F_{2c}\right)^2. \tag{5.23}$$

Inserting Eqs. (5.23) into (5.17) to eliminate the critical contact half-width, we can obtain a governing equation to solving the pull-off force as

$$1 = \left(\frac{A\left(1+n\right)^2}{\pi\gamma\left(\delta+n\right)\left(\overline{\delta}+n\right)}\right)^{n+1} \frac{\left(F_{2c}\right)^{2n+1}\cosh \pi\varepsilon}{2^{2n+1}\left(\varepsilon^2+\frac{1}{4}\right)A} \left\{ \begin{array}{l} \left(1+n\right)\varepsilon\int_0^1 \left[d_n \cos\left(\varepsilon\ln\frac{T+1}{1-T}\right) - c_n \sin\left(\varepsilon\ln\frac{T+1}{1-T}\right)\right]\frac{T^n}{\sqrt{1-T^2}}dT \\ +\left(\varepsilon^2-\frac{1}{4}-\frac{1}{2}n\right)\int_0^1 \left[c_n \cos\left(\varepsilon\ln\frac{T+1}{1-T}\right) + d_n \sin\left(\varepsilon\ln\frac{T+1}{1-T}\right)\right]\frac{T^{n+1}}{\sqrt{1-T^2}}dT \end{array} \right\}$$
$$. \tag{5.24}$$

Now let's exemplify two simple cases: the wedge non-slipping contact ($n=0$) and the non-slipping Herzian contact ($n=1$).

For the wedge non-slipping contact ($n=0$), from Eq. (5.24), we have

$$F_{2c} = -\frac{\pi\gamma}{2c_0} \left[1 + \left(4 - \frac{\pi^2}{2}\right)\varepsilon^2 + O\left(\varepsilon\right)^3\right] \approx \frac{\pi\gamma}{2\phi} \left(1 - 0.9348\varepsilon^2\right). \tag{5.25}$$

For the non-slipping Herzian contact ($n=1$), similarly from Eq. (5.24), we have

$$F_{2c} = -\frac{3}{2} \left(\frac{\pi\gamma^2}{Ac_1}\right)^{\frac{1}{3}} \left\{1 + \frac{8}{27}\left(2 - 3\text{Catalan}\right)\varepsilon^2 + O\left(\varepsilon\right)^3\right\} \approx \frac{3}{2} \left(\frac{\pi\gamma^2 R}{A}\right)^{\frac{1}{3}} \left(1 - 0.2216\varepsilon^2\right). \tag{5.26}$$

Clearly, the pull-off force of two-dimensional JKR model can be achieved by setting $\varepsilon=0$ in Eq. (5.26). It can be ascertained from Eqs. (5.25) and (5.26) that the pull-off forces of non-slipping adhesive contacts are smaller than the corresponding solutions

of frictionless models ($\varepsilon = 0$). Because $|\beta| \leq 1/2$ for an arbitrary bi-material combination, we may find $|\varepsilon|^2 \leq \left(-\frac{1}{2\pi} \ln 3 \right)^2 \approx 0.03057$ from Eq. (3.5). This implies that the influence of the *interface mismatch eigenstrain* on the pull-force is quite limited and the adhesive contacts can be approximately modelled by frictionless contact models.

6. Concluding remarks

The problems of non-slipping contact between dissimilar elastic solids have been studied under the plane strain theory. Separately considering the situations with and without surface adhesive effect, the *interface mismatch eigenstrain* has been derived for non-slipping contacts with symmetric indenter profile. Its explicit expressions enable the boundary-value problems to be thoroughly analyzed and addressed. In details, it laid a foundation for fretting fatigue analysis for the contacts at the macro-scale. At the same time, it theoretically validated the application of frictionless adhesive contact models at micro-, and nano- scales.

It is expected that the solutions developed in this paper can be useful for the further modeling non-slipping contacts elsewhere.

Acknowledgements

References

1. Arzt, E., Gorb, S., Spolenak, R., 2003. From micro to nano contacts in biological attachment devices, Proc. Natl. Acad. Sci. USA, 100, 10603-10606.

2. Barber, J.R. 2018. Contact mechanics, Springer, New York

3. Bhushan, B., 2017. Depth-sensing nanoindentation measurement techniques and applications, Microsyst. Technol. 23:1595-1649.

4. Borodich F. M. and Keer, L. M. 2004, Evaluation of elastic modulus of materials by adhesive (no-slip) nano-indentation. Proc. R. Soc. Lond. A 2004 460, 507-514.

5. Borodich, F.M., Galanov, B.A., Keer, L.M., Suarez-Alvarez, M.M. 2021. Contact probing of prestressed adhesive membranes of living cells. Phil. Trans. R. Soc. A

379, 20200289

6. Dartsch, P.C., Hammerle, H., 1986. Orientation response of arterial smooth muscle cells to mechanical stimulation. Eur. J. Cell Biol. 41, 339-346.

7. England, A.H., 1971. Complex variable methods in elasticity. John Wiley & Sons Ltd. London.

8. Erdogan, F., Gupta, G.D., Cook, T.S., 1973. Numerical solution of singular integral equation. In: Sih, G.C. (Ed.), Methods of Analysis and Solutions of Crack Problems, Noordhoff: Groningen, pp. 368-425.

9. Galin, L. A., 1953. Contact problems in the theory of elasticity, Gostekhizdat, Moscow-Leningrad (English translation by H. Moss, edited by I. N. Sneddon, North Carolina State College, Departments of Mathematics and Engineering Research, NSF Grant No. G16447, 1961).

10. Gladwell, G. M. L., 1980. Contact Problems in the Classical Theory of Elasticity, Sijthoff & Noordhoff, Alphen aan den Rijn, the Netherlands.

11. Goodman, L.E., 1962. Contact stress analysis of normally loaded rough spheres. J. Appl. Mech. 29, 515-522.

12. Hertz, H., 1881. On the contact of elastic solids. J. Reine und Anges. Math. 92, 147-152.

13. Hills, D.A., Nowell, D., Sackfield, A., 1993. Mechanics of Elastic Contact. Butterworth-Heinemann Ltd.

14. Johnson, K.L., 1985. Contact mechanics. Cambridge University Press.

15. Johnson, K.L., Kendall, K., Roberts, A.D., 1971. Surface energy and the contact of elastic solids. Proc. Roy. Soc. Lond. A 324, 301-313.

16. Luan, B., Robbins, M.O., 2006. Contact of single asperities with varying adhesion: Comparing continuum mechanics to atomistic simulations. Phy. Rev. E 74, 026111.

17. Ma, L., Korsunsky, A.M, 2006. The analytical solution for sliding rounded-edge contact, J. Elast. 82, 9-30.

18. Ma, L., Korsunsky, A.M, 2012. Complex variable formulation for non-slipping plane strain contact of two elastic solids in the presence of interface mismatch eigenstrain, International Journal of Solids and Structures 49,177-188.

19. Malyshev, B.M. and Salganik, R.L. (1965). The strength of adhesive joints using the theory of crack. International Journal of Fracture Mechanics 1, 114-128.

20. Mossakovski, V.I., 1954. The fundamental general problem of the theory of

elasticity for a half-space with a circular curve determining boundary conditions. Appl. Math. Mech. 18, 187-196 (in Russian).

21. Mossakovski, V.I., 1963. Compression of elastic bodies under conditions of adhesion (axisymmetric case).   Appl. Math. Mech. 27, 418-427.

22. Muskhelishvili, N.I., 1953. Some basic problems of the mathematical theory of elasticity. Noordhoff, Groningen.

23. Nowell, D., Hills, D.A., Sackfield, A., 1988. Contact of dissimilar elastic cylinders under normal and tangential loading. J. Mech. Phys. Solids **36**, 59-75.

24. Soldatenkov I.A., 1996. Indentation with adhesion of a symmetrical punch into an elastic half-plane. J. Appl. Math. Mech. 60 (2), 261-267.

25. Spence, D.A., 1968. Self-similar solutions to adhesive contact problems with incremental loading. Proc. Roy. Soc. Lond. A 305, 55-80.

26. Spence, D.A., 1973. An eigenvalue problem for elastic contact with finite friction, Proc. Camb. Phil. Soc. 73, 249-268.

27. Spence, D.A.,1975. The Hertz contact problem with finite friction, Journal of Elasticity, 5, 297-319.

28. Szegö, G.., 1975. Orthogonal polynomials, American Mathematical Society, Providence, Rhode Island.

29. Yang, S., Saif, T., 2005. Reversible and repeatable linear local cell force response under large stretches. Exp. Cell Res. **305**, 42-50.

30. Zhupanska, O.I., Ulitko, A.F., 2005. Contact with friction of a rigid cylinder with an elastic half-space. J. Mech. Phys. Solids 53, 975-999.

Appendix: Singular integrals

Some singular integrals are frequently encountered in contact mechanics. One representative form of singular integrals is

$$I_1(x) = \frac{1}{\pi} \int_{-1}^{1} \frac{(1-t)^\alpha (1+t)^\beta Q_1(t)}{t-x} dt, \quad (-1 < x < 1) \tag{A1}$$

where $-1 < \mathrm{Re}(\alpha, \beta) < 1, \alpha + \beta = \pm 1, 0$, and $Q_1(t)$ can be any polynomial expression. Formula (A1) should be understood in the sense of Cauchy principal value or Hadamard finite part integration if required. Integral (A1) will be inevitably involved in all non-slipping contact solutions.

The following formula for Jacobi polynomials is found powerful in solving the above integral (Erdogan et al, 1973; Ma and Korsunsky, 2006):

$$\frac{1}{\pi}\int_{-1}^{1}\frac{(1-t)^{\alpha}(1+t)^{\beta}P_{n}^{(\alpha,\beta)}(t)}{t-x}dt=\cot(\pi\alpha)(1-x)^{\alpha}(1+x)^{\beta}P_{n}^{(\alpha,\beta)}(x)-\frac{2^{(\alpha+\beta)}}{\sin\alpha\pi}P_{n+(\alpha+\beta)}^{(-\alpha,-\beta)}(x) \quad \text{(A2)}$$

where $\mathrm{Re}(\alpha,\beta)>-1, \alpha+\beta=\pm1,0; \alpha\neq0,1$, and the Jacobi polynomials are defined from the hypergeometric function as (Szegö, 1975)

$$P_{n}^{(\alpha,\beta)}(z)=\frac{\Gamma(\alpha+1+n)}{\Gamma(\alpha+1)\Gamma(n+1)}F\left(-n,1+\alpha+\beta+n;\alpha+1;\frac{1-z}{2}\right). \quad (n\geq0) \qquad \text{(A3)}$$

From this definition, one can find

$$P_{n}^{(\alpha,\beta)}(t)=0, \quad (n<0) \qquad \qquad \text{(A4)}$$

and

$$P_{0}^{(\alpha,\beta)}(t)=1$$

$$P_{1}^{(\alpha,\beta)}(x)=(\alpha+1)+\frac{(\alpha+\beta+2)}{2}(x-1)$$

$$P_{2}^{(\alpha,\beta)}(x)=\frac{(\alpha+1)(\alpha+2)}{2}+\frac{(\alpha+2)(\alpha+\beta+3)}{2}(x-1)+\frac{(\alpha+\beta+3)(\alpha+\beta+4)}{2}\left(\frac{x-1}{2}\right)^{2}$$

$$P_{i}^{(\alpha,\beta)}(x)=...(i=2,3,...n)$$

.(A5)

The recurrence relation for the Jacobi polynomials is

$$P_{n}^{(\alpha,\beta)}(x)=\frac{(2n+\alpha+\beta-1)\{(2n+\alpha+\beta)(2n+\alpha+\beta-2)x+\alpha^{2}-\beta^{2}\}}{2n(n+\alpha+\beta)(2n+\alpha+\beta-2)}P_{n-1}^{(\alpha,\beta)}(x)$$

$$-\frac{2(n+\alpha-1)(n+\beta-1)(2n+\alpha+\beta)}{2n(n+\alpha+\beta)(2n+\alpha+\beta-2)}P_{n-2}^{(\alpha,\beta)}(x) \quad \text{(A6)}$$

$$(n=2,3,...)$$

and

$$P_{n}^{(\alpha,\beta)}(-x)=(-1)^{n}P_{n}^{(\beta,\alpha)}(x). \qquad \qquad \text{(A7)}$$

Now suppose that the polynomial $Q_{1}(t)$ in (A1) can be expanded into a series of Jacobi polynomials in the form

$$Q_{1}(t)=\sum_{n=0}^{\infty}d_{n}P_{n}^{(\alpha,\beta)}(t). \qquad \qquad \text{(A8)}$$

The coefficients d_{n} can be determined by Jacobi polynomial's orthogonal relationship

$$\int_{-1}^{1}(1-t)^{\alpha}(1+t)^{\beta}P_{m}^{(\alpha,\beta)}(t)P_{n}^{(\alpha,\beta)}(t)dt=\frac{2^{\alpha+\beta+1}}{(2n+\alpha+\beta+1)}\frac{\Gamma(n+\alpha+1)\Gamma(n+\beta+1)}{\Gamma(n+\alpha+\beta+1)\Gamma(n+1)}\delta_{mn} \quad \text{(A9)}$$

as

$$d_n = \frac{(2n+\alpha+\beta+1)}{2^{\alpha+\beta+1}} \frac{\Gamma(n+\alpha+\beta+1)\Gamma(n+1)}{\Gamma(n+\alpha+1)\Gamma(n+\beta+1)} \int_{-1}^{1} Q_1(t)(1-t)^{\alpha}(1+t)^{\beta} P_n^{(\alpha,\beta)}(t)dt. \quad (A10)$$

Inserting (A8) into (A1), one can find the general solution as

$$I_1(x) = \frac{1}{\pi} \int_{-1}^{1} \frac{(1-t)^{\alpha}(1+t)^{\beta} Q_1(t)}{t-x} dt$$

$$= \cot(\pi\alpha)(1-x)^{\alpha}(1+x)^{\beta} Q_1(x) - \frac{2^{(\alpha+\beta)}}{\sin\alpha\pi} \sum_{n=0}^{\infty} d_n P_{n+(\alpha+\beta)}^{(-\alpha,-\beta)}(x) \qquad . (-1<x<1) \quad (A11)$$

This implies that if $Q_1(t)$ is a finite polynomial, the closed-form analytical solution

of $I_1(x)$ can be obtained.

Additionally, from the formula (A11), the following two identities can be derived

$$\frac{1}{\pi} \int_{-1}^{1} \frac{(1-t)^{\alpha}(1+t)^{\beta}}{t-x} dt = \cot(\pi\alpha)(1-x)^{\alpha}(1+x)^{\beta} - \frac{2^{(\alpha+\beta)}}{\sin\alpha\pi} P_{(\alpha+\beta)}^{(-\alpha,-\beta)}(x), (-1<x<1) \quad (A12)$$

$$\frac{1}{\pi} \int_{-1}^{1} \frac{t(1-t)^{\alpha}(1+t)^{\beta}}{t-x} dt = \cot(\pi\alpha)(1-x)^{\alpha}(1+x)^{\beta} x$$

$$- \frac{2^{\alpha+\beta}}{\sin\alpha\pi} \left[\frac{2}{\alpha+\beta+2} P_{1+\alpha+\beta}^{(-\alpha,-\beta)}(x) + \frac{\beta-\alpha}{\alpha+\beta+2} P_{\alpha+\beta}^{(-\alpha,-\beta)}(x) \right] \qquad , (-1<x<1). \quad (A13)$$